Astrophys. Space Sci. Trans., 7, 327–333, 2011
www.astrophys-space-sci-trans.net/7/327/2011/
doi:10.5194/astra-7-327-2011

ASTRA
Astrophysics and Space Sciences Transactions

Cosmic ray composition studies through the Gerasimova-Zatsepin effects of heavy nuclei at LAAS

A. Iyono[1], H. Matsumoto[1], K. Okei[2], S. Tsuji[2], S. Ohara[3], N. Ochi[4], T. Konishi[5], N. Takahashi[6], I. Yamamoto[7], T. Nakatsuka[8], T. Nakamura[9], N. Ohmori[9], and K. Saitoh[10]

[1]Dept. of Fundamental Science, Okayama University of Science, Okayama 700-0005, Japan
[2]Kawasaki Medical School, Kurashiki 701-0192, Japan
[3]Nara University of Industry, Nara 636-8503, Japan
[4]Yonago National College of Technology, Tottori 683-8502, Japan
[5]Kinki University, Osaka 577-8502, Japan
[6]Hirosaki University, Hirosaki 036-8561, Japan
[7]Dept. of Information and Computer Engineering, Okayama University of Science, Okayama 700-0005, Japan
[8]Okayama Shoka University, Okayama 700-8601, Japan
[9]Kochi University, Kochi 780-8520, Japan
[10]Ashikaga Institute of Technology, Ashikaga 326-8558, Japan

Received: 14 November 2010 – Revised: 1 March 2011 – Accepted: 23 March 2011 – Published: 1 September 2011

Abstract. Extensive air showers (EASs) originated from primary cosmic ray energies above 10^{15} eV have been measured at multiple EAS observatories deployed in Japan since Sept. 1996. The typical EAS array has been located at the rooftop of the buildings in the university campus, and has GPS-disciplined 10 MHz oscillator to provide the UTC time stamp for each EAS event within a few μs accuracies. Searching for simultaneous and parallel EAS events at multiple EAS observatories due to Gerasimova-Zatsepin (GZ) effects have been carried out by comparing EAS arrival time stamps and directions detected by several baseline combinations of EAS arrays.

The EAS pairs whose time difference and angular distance were less than 5 ms and less than 15°respectively, were selected and their angular distances from the solar direction and the lunar direction were examined. The data were compared with numerical GZ probability as a function of arrival directions of cosmic ray nuclei. Consequently, significant excesses of these events in the solar direction as expected in the numerical prediction of GZ effects were not found. We however found that the deficiencies of EAS pairs in the lunar direction, but its deviation is not significant.

Correspondence to: A. Iyono
(iyono@das.ous.ac.jp)

1 Introduction

The origin, acceleration mechanism and propagation processes of ultra-high energy cosmic rays has been a fundamental question for many decades, and it still is an unresolved mystery in the field of high energy astrophysics. Above the cosmic ray primary energies of 10^{15} eV, direct measurements of cosmic ray energy and identifications of cosmic ray particle species have been impossible. In order to estimate their energy and mass compositions, the EAS observations at the sea level or high altitude mountains have been carried out. In these experiments, statistical approaches to derive cosmic ray composition are used. But, these approaches depends on the hadron interaction model because accelerator data are not available in these ultra-high energies.

The alternative approach to derive the mass composition of cosmic rays is as follows. The photo-disintegration process of cosmic ray nuclei with solar visible photons ~ 1 eV, allows directly exploring the mass composition of cosmic ray at energies above 10^{18} eV, if the multiple EAS events due to fragment particles can be registered simultaneously at several EAS arrays and the energy of each EAS can be estimated. This idea was originally suggested by Zatsepin and Gerasimova and this process is known as the Gerasimova-Zatsepin (GZ) effect (Zatsepin, 1950; Gerasimova and Zatsepin, 1960).

Published by Copernicus Publications on behalf of the Arbeitsgemeinschaft Extraterrestrische Forschung e.V.

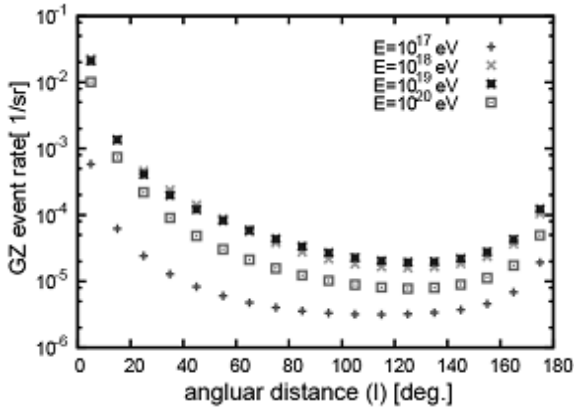

Fig. 1. The GZ probability distribution as a function of the angular distance of cosmic ray iron nuclei from the solar direction. The symbols (+), (x), (*) and (□) represent the primary energies: $10^{17}, 10^{18}, 10^{19}and10^{20}$ eV respectively.

1.1 Numerical approaches

Several numerical approaches (MedinaTance and Watson, 1999; Epele et al., 1999; Fujiwara et al., 2006; Lafébre et al., 2008) have been carried out in order to study the observation possibilities of GZ originated EAS events by using EAS arrays at the earth. In these calculations, the photodisintegration cross section, fragmentation cross section and propagations of fragments in the interplanetary magnetic field according to their magnetic rigidity were taken into account. They predicted the separation distance between EAS events at arriving the earth's surface.

Lafébre et al. (Lafébre et al., 2008) reported the absolute GZ energy spectrum and the fraction of the integral primary cosmic ray spectrum above 10^{16} eV. They concluded the maximum GZ probability $\sim 10^{-4}$ near 1.5×10^{18} eV if their EAS separation distances should be less than one Earth diameter. The separation distance distributions of GZ EAS events arriving at the earth's surface were also reported in Lafébre et al. (2008); Fujiwara et al. (2006). For instance, the expected separation distance for primary iron nuclei of 10^{18} eV were expected as 1000 km. Lafébre et al. parametrized the average separation distance $\langle\delta\rangle$ as a function of primary cosmic ray energy E in Lafébre et al. (2008),

$$\langle\delta\rangle = 4A \left| \frac{Z_1}{A_1} - \frac{Z_2}{A_2} \right| (\frac{10^{19}\text{eV}}{E}) \text{ km}$$

where Z_1 and Z_2 represent the charge of fragments, and A_1 and A_2 do their mass number, respectively. A is the mass number of primary cosmic ray nuclei.

The other feature of GZ originated EAS events is that the probability distributions of GZ events strongly depends on the arrival directions. The angle α between the directions of propagation of the cosmic ray nuclei and of the solar photons determined the GZ probability distribution. When cosmic rays came from the solar direction or the anti-solar direction, which means daytime or nighttime observations respectively, the GZ probabilities are enhanced. Our numerical predictions were shown in Fig. 1. These probabilities enhanced around the solar direction and anti-solar direction. This means daytime and nighttime observations are more effective for GZ events. But Lafébre et al. (2008) also reported that due to the complexity of the solar magnetic field near the Sun the fragment trajectories would deviate very largely. Therefore the night side observations are to be expected to provide highest event rates.

From the view point of experimental setup to identify GZ events, the most important key observables are the coincidence of the EAS arrival timing and the same direction of EASs observed at multiple and distant EAS sites separated by 100 km or more. The other important observable is the threshold energy of each EAS array. While the photodisintegration process of cosmic ray nuclei with solar photon could occur above their energies of 10^{18} eV, the energies of fragments should be less than several $\times 10^{17}$ eV. This energy threshold required that the detector spacing should be much less than 1 km at each EAS site.

The Large Area Air Shower (LAAS) experiments (Ochi et al., 2003) have been established in order to study large-scale correlations in ultra-high energy cosmic rays by Kitamura (Kitamura et al., 1997) in 1995. And the LAAS EAS arrays are scattered over in Japan and are located at the sea-level atmospheric depth, and they have been operated since 1996. These arrays have been synchronized with each other within the accuracy of one microsecond by using GPS-disciplined UT time stamp system. This system enables to observe simultaneous and parallel EAS events at multiple EAS arrays. The threshold energy of primary cosmic rays in our array is around PeV. Thus, LAAS experiments are suitable for investigating the GZ events.

This paper describes the LAAS experimental apparatus briefly. The results of data analysis for identifying the GZ candidate events are discussed with some numerical results.

2 LAAS experiments

2.1 Array setup

The LAAS experiments (Ochi et al., 2003) are the joint projects of compact EAS arrays maintained at several institutes in Japan. These arrays are scattered over Japan from 34° N to 40° N and 134° E to 140° E shown in Fig. 2. Those mutual baselines are ranging from 0.1 km to 1000 km. The geographical location and mutual distances from the specified EAS arrays are listed in Table 1. In the fifth to the seventh columns of Table 1, we specified mutual distances measured from HU, KU and OUS sites respectively.

In each institute, the EAS arrays are located at the rooftop of buildings in university campus. The array typically con-

Table 1. The geographical location and mutual distances between LAAS EAS arrays

Institute	Abbreviation	Latitude(N)	Longitude(E)	Distance[km] from HU	KU	OUS
Hirosaki University	HU	°40 35'	°140 29'	-	787	872
Kinki University+	KU	°34 39'	°135 36'	787	-	152
Nara University of Industry	NUI	°34 35'	°135 41'	788	11	161
Okyama University*	OU	°34 41'	°133 55'	873	153	1
Okyama University of Science	OUS	°34 42'	°133 56'	872	152	-

+:moved to NUI and * :moved to OUS in 2008.

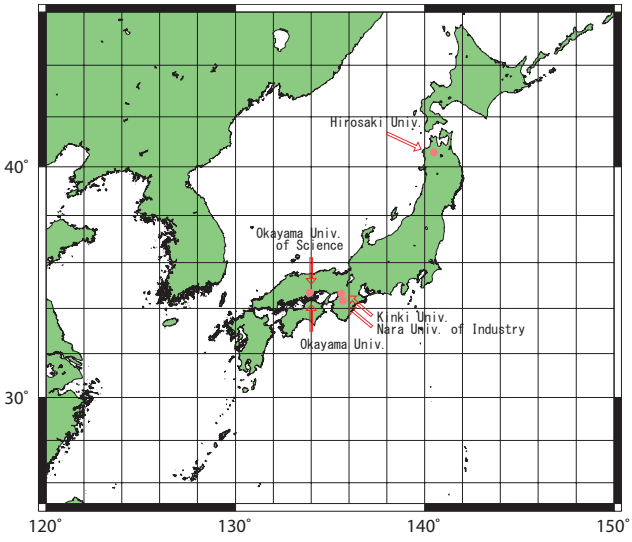

Fig. 2. The geographical map of LAAS EAS arrays in Japan. The symbols (•) represent the location of EAS arrays and the institution names are also shown.

sists of eight plastic scintillation detectors whose size is $50 \times 50\,\mathrm{cm}^2 \times 5\,\mathrm{cm}$. The detectors are deployed over a rooftop area of approximately $200\,\mathrm{m}^2$.

The data acquisition system is triggered when each of more than 3 detectors are hit within 100ns time window. The relative arrival times of EAS front particles are digitized with a CAMAC TDC (Kaizuworks Model 3780) with the resolution of 40 ps. The local density of EAS particles is digitized with a CAMAC ADC (Lecroy Model 2249W), of which dynamic range is limited to less than 10 particles. The typical trigger frequency is about 0.1 to 0.5 Hz at each array. The time stamp of each EAS event is registered by using a CAMAC GPS timing module (Kaizuworks Model 3850A), which maintains GPS-disciplined TCXO of 10 MHz frequency. The accuracy of UT time stamp is 1μs at each EAS array.

The EAS arrival direction is determined by fitting a plane to EAS particle arrival times calculated from TDC values. It is unlikely that the EAS core location and shower size could be obtained, because of the limitation of EAS array sizes and ADC dynamic ranges. Thus, the arrival direction angle and UT time stamp of each EAS event are analyzed in the following physics analysis.

Table 2. LAAS EAS arrays in Okayama area

Array	ND	Area [m^2]	NE Nc≥ 3	Event rate[s^{-1}] Nc≥ 3
OU	8	15×25	1.9×10^6	3.05×10^{-2}
OUS1	8	8×15	2.4×10^6	3.69×10^{-2}
OUS2	8	25×31	2.1×10^6	3.61×10^{-2}
OUS3	5	8×8	1.5×10^6	3.23×10^{-2}

ND: number of scintillation detectors.
NE: number of events
Nc: the applied cut on the number of coincidences.

2.2 LAAS arrays in Okayama area

The LAAS group has operated four EAS arrays in Okayama University (OU) and Okayama University of Science (OUS). One array was set up in the campus of OU and three arrays have been deployed in that of OUS which are abbreviated as OU, OUS1, OUS2 and OUS3, respectively. The distance between OU array and OUS arrays is almost 1 km, and the mutual distances between OUS arrays are about one hundred meter. It was expected that ultra-high energy EAS might be detected by both OU array and some of OUS arrays, and relatively higher energy EAS could hit multiple EAS arrays among the OUS arrays. To confirm the array performance and detection energy range, we searched for coincident EAS events within OU and OUS arrays in the window of the difference of each EAS arrival time. The data sets analyzed here, are also summarized in Table 2. To identify EAS data from raw data, it was applied that the number of coincidences Nc was greater than 3 (Nc≥3).

Though it is unable to determine the shower size parameter for each event by using a compact EAS array in LAAS,

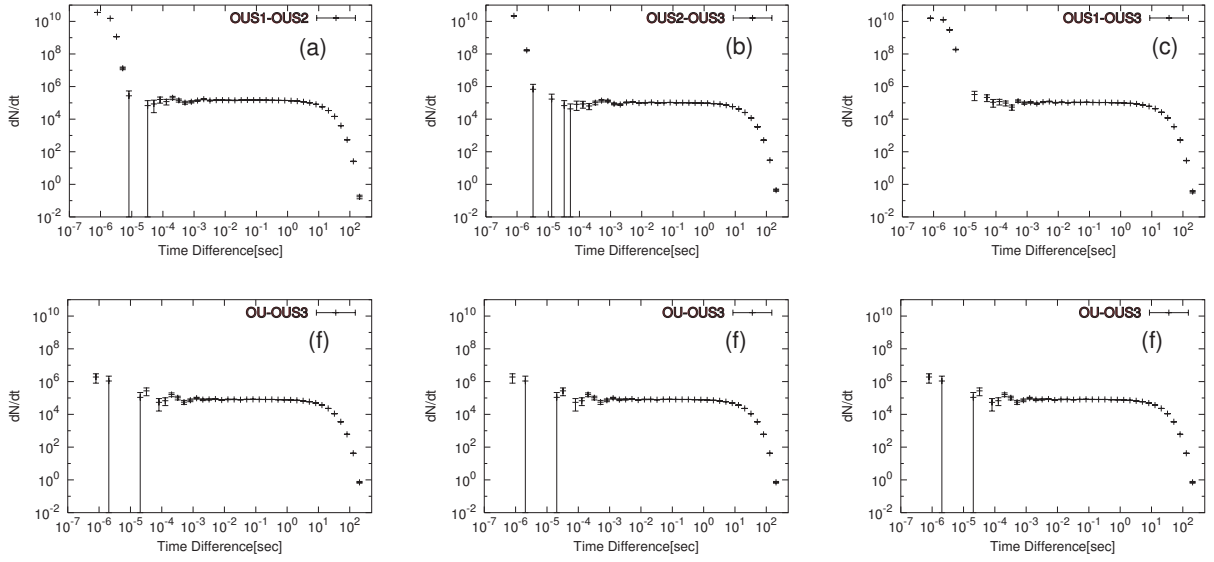

Fig. 3. Time difference distributions for OUS-OUS and OU-OUS EAS array combinations: **(a)** OUS1-OUS2, **(b)** OUS2-OUS3, **(c)** OUS3-OUS1 for about 100 m baseline combinations and **(d)** OU-OUS1, **(e)** OU-OUS2, **(f)** OU-OUS3 for about 1000 m baseline combinations.

Table 3. The number of events observed at several array combinations in Okayama area

	Baseline [m]	Number of events	Event rate [s^{-1}]
OUS1-OUS2	101	70.2k	1.1×10^{-3}
OUS2-OUS3	127	35.5k	7.1×10^{-4}
OUS3-OUS1	114	38.6k	7.8×10^{-4}
OU-OUS1	1139	3	9.3×10^{-8}
OU-OUS2	1036	9	3.1×10^{-7}
OU-OUS3	1116	4	1.2×10^{-7}

Data period [days]:
OUS1-OUS2:713, OUS2-OUS3:566, OUS3-OUS1:564
OU-OUS1:373, OU-OUS2:338, OU-OUS3:396.

it is possible to select shower size ranges in a way by requiring coincidences at multiple EAS arrays of the four arrays located in Okayama area. The time difference of EAS events between two arrays were calculated in order to find simultaneous EAS events which hit multiple EAS sites. It can be expected that time difference distributions of EAS pairs are well expressed as an exponential distribution because most of EAS events arrive randomly in the time order. Consequently, time difference distributions can be expressed well as exponential function. The obtained time difference distributions are shown in Fig. 3. Because these time difference distributions represented the number of events per fixed step size in the time bin, those exponential function drops very rapidly above 1 s on a log-log scale in Fig. 3. When the time differences are very small, exponential function becomes constant if all EAS pairs came from random coincidences. However, it is apparent that the significant excess of event rates was found at around 10 µs in OUS-OUS combinations and OU-OUS combinations shown in Fig. 3. These excesses came from non-random coincidence EAS events, which hit multiple EAS arrays simultaneously. Taking account of the experimental resolution of GPS system, EAS front structures, and the baseline of array combinations, the EAS event pairs within 3 µs are defined as a single EAS event. The numbers of events obtained under these criteria from all combinations of arrays are summarized in Table 3. The baseline distances of each combination are also listed in the same table.

2.3 Array performance and results

To understand the performance of each array, the Monte Carlo simulations were made on the basis of modified Nishimura-Kamata-Grisen's lateral functions of electron components with an energy threshold parameter equal to 5 MeV and muon components (Ochi et al., 2003). The primary cosmic ray compositions are assumed as the mixture of 90% protons and 10% iron nuclei. The detectable angular range of the EASs is less than 45°in LAAS arrays. The spectral indices of primary cosmic ray energy are assumed as -2.7 below $10^{15.6}$ eV and -3.2 above this energy.

The effective areas both in a single EAS array case and multiple array cases, were simulated under the condition required for EAS data acquisition and off-line analysis. The primary energy response functions were obtained and the results are summarized in Table 4. For the single array, the observed primary energy ranges from 0.1 to 1.8×10^{15} eV. And the primary energy of EAS which were detected simul-

Table 4. Performance of LAAS EAS array in Okayama area.

EAS array	Median primary energy[eV]	FWHM[eV]	Event Rate per day	
			Simulation	Observed
OU	6.3×10^{14}	$8.3\times10^{13}-1.8\times10^{15}$	4630	2634
OUS1	5.3×10^{14}	$9.0\times10^{13}-1.2\times10^{15}$	5510	3188
OUS2	6.3×10^{14}	$8.3\times10^{13}-1.8\times10^{15}$	4650	3119
OUS3	5.3×10^{14}	$8.5\times10^{13}-1.4\times10^{15}$	2630	2796
OUS1-OUS2	9.2×10^{15}	$2.4\times10^{15}-1.9\times10^{16}$	70	98
OUS2-OUS3	1.4×10^{16}	$3.6\times10^{15}-3.2\times10^{16}$	17	61
OUS3-OUS1	1.1×10^{16}	$3.0\times10^{15}-2.6\times10^{16}$	25	66
OU-OUS1	6.9×10^{18}	$1.2\times10^{18}-1.8\times10^{19}$	3.7×10^{-3}	8.0×10^{-3}
OU-OUS2	5.5×10^{18}	$9.9\times10^{17}-1.3\times10^{19}$	5.1×10^{-3}	2.7×10^{-2}
OU-OUS3	6.5×10^{18}	$1.2\times10^{18}-1.7\times10^{19}$	2.0×10^{-3}	1.0×10^{-2}

taneously in OUS and OUS combinations is one order of magnitude greater than that obtained by the single array, and ranges from 3×10^{15} eV to 3×10^{16} eV. By using the OU and OUS array combinations, we can select EAS events whose energies are above 1EeV. Therefore these single or multiple array combinations allow obtaining the cosmic ray intensity spectrum. The observed event rates are compared with this simulation results, shown in Table 4. In Fig. 4, the obtained integral spectrum was shown with simulated results. The data points determined by single array and OUS and OUS combinations are well described by $E^{-1.7}$. The spectral index of OU and OUS combinations is approximately -2.2. Although statistics are still poor in the highest data points, spectral indices obtained by LAAS experiments are in agreement with expected.

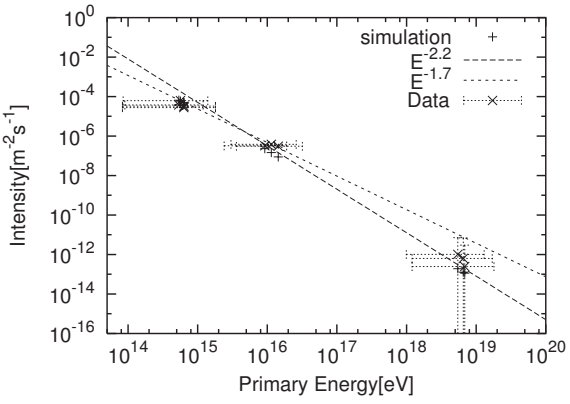

Fig. 4. Integral energy spectrum. The symbols (x) and (+) represents obtained data and simulation results, respectively.

3 Data Analysis

In order to select simultaneous EAS events at multiple EAS sites within 1 km baseline in Okayama area, the analysis of time differences of EAS pairs are used which is described in Sect. 2.2. By applying these procedures to LAAS long baseline observations and adopting event selection criteria predicted by numerical approaches, it will enable to identify simultaneous EAS events at long baseline EAS sites. Therefore, we have applied the following event selection criteria for our observation data:

1. the number of coincidence counters was larger than 5 corresponding to the threshold energy of 5 PeV,
2. the baseline lengths were limited to 100 km or more,
3. the time difference of EAS events were smaller than 5 ms which came from the mutual geographical locations of EAS sites,
4. the angular distances of EAS events were less than 15°, because the angular resolution of EAS arrays is about 7°.

The data period is from Sept. 1996 to Dec. 2006, and total number of events is about 65 M and the accumulated exposure time is 11 k days.

4 Results

To obtain the candidates of GZ events, the condition described in Sect. 3 are set for data analysis. In the case of the long baselines such as 870 km between OU or OUS arrays and HU array and 160 km between OU or OUS arrays and KU or NUI arrays, time difference distributions are presented in Fig. 5. In these figures, fitted exponential functions are also shown. These exponential decreasing is expected from

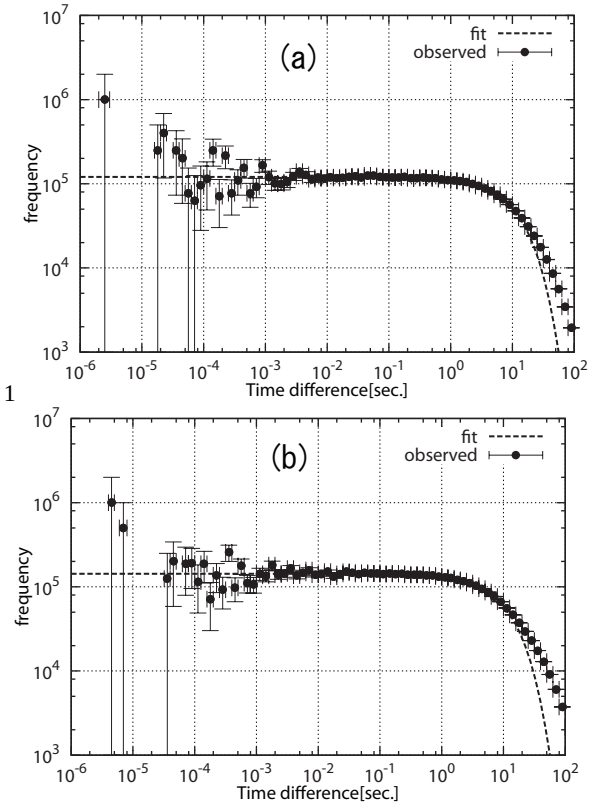

Fig. 5. Time difference distributions. **(a)** long baseline cases (870 km). **(b)** midrange baseline cases (160 km). Dashed lines represent fitted exponential functions due to randomness of EAS arrival time distributions.

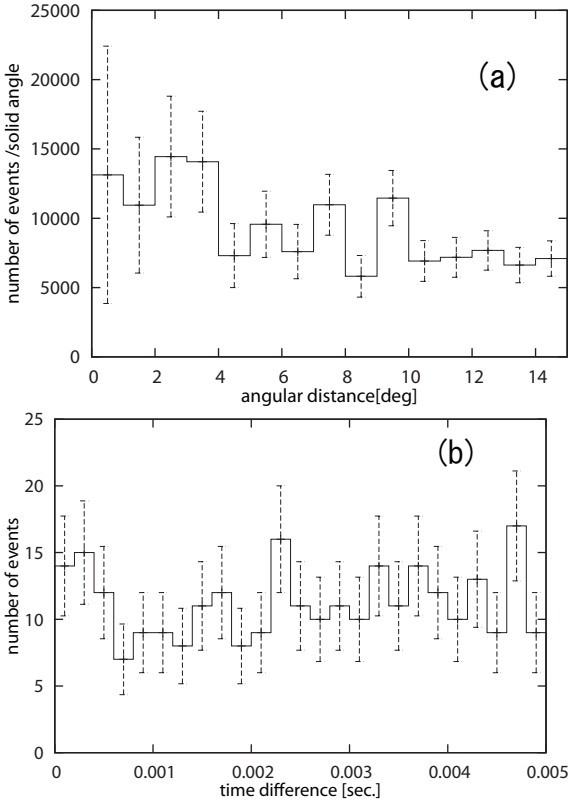

Fig. 6. **(a)** The angular distance distribution and **(b)** the time difference distribution between the selected EAS pairs.

the randomness of EAS arrival time distributions. The differences between data and fitted exponential functions are enhanced above the time difference of 10 s because of the accidental or maintenance operation discontinuances of the EAS arrays. In the time difference range from ms to 10 s, data are well described by exponential functions, which mean random coincidences of EAS pairs. While data are fluctuated statistically, excessive of the EAS pairs are observed in the time range below several ms time differences. The limitation of angular resolution of EAS arrays causes some ambiguity on time differences which came from the geographical arrangement of EAS arrays. Thus, we selected events in the time difference ranging up to 5 ms.

After applying the criteria described above, the distributions of the angular distance and time difference between EAS pairs are obtained and shown in Fig. 6. The value of the reduced χ^2 for uniform angular distance distribution is $\chi^2_\nu/DOF = 26.6/14$. In Fig. 6**(b)**, $\chi^2_\nu/DOF = 8.4/14$. Both distributions agree to uniform distributions.

The probability of GZ event observation depends on the angle between the directions of propagation of cosmic ray nuclei and of the solar photons and these increases near both solar and anti-solar directions. According to the GZ scenarios, we calculated the angular distance of selected EAS pairs from the solar direction. The obtained angular distance distributions are shown in Fig. 7**(a)**. The GZ standard scenario predicted the probability maximum in the solar directions, but our results show the uniform distribution rather than the excesses in the solar direction as well as in the anti-solar direction. The angular distance distribution of selected GZ candidate events seems to be uniform compared with Fig. 1.

Another apparent obstacle of very high energy cosmic ray stream is the moon reported in Tibet (Amenomori et al., 2007), L3 (Achard et al.,, 2005) and ARGO-YBJ (Wang et al., , 2008) and some other experiments. The distribution of angular distances from the lunar direction is shown in Fig. 7**(b)**. The present result suggests the existence of some deficiencies from the uniform distribution around the lunar direction. The significance level, however, is still less than two standard deviation, so that we cannot conclude any more for these phenomena.

5 Conclusions

LAAS experiments have carried out EAS observations by using GPS synchronized EAS arrays. By using the array in Okayama area, we have determined the integral energy spec-

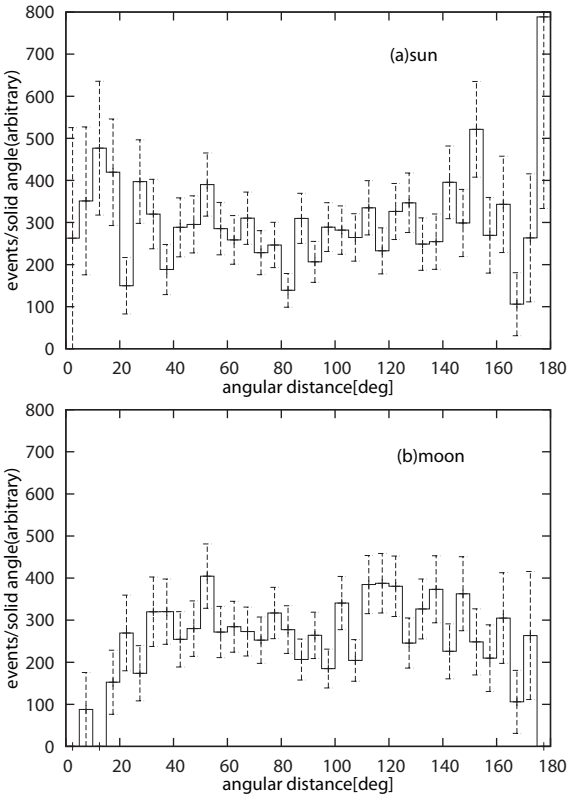

Fig. 7. The angular distance distribution between each direction of the selected EAS events and **(a)** the solar and **(b)** the lunar directions.

trum of cosmic rays when applying the time difference distribution analysis for EAS pairs. The extension of energy spectrum analysis to long baseline EAS sites allows searching simultaneous and parallel EAS events. Using LAAS's one decade observation data, we have selected EAS events like Gerasimova-Zatsepin effects under the limitation of angular and time differences of EAS pairs.

We compare obtained angular distance distributions from solar direction with numerical one. The apparent excess in solar direction and anti-solar direction was not found, and the distribution seems to be uniform. On the other hand, the correlation between GZ like events and lunar direction indicates somewhat deficiencies in small angular distances, but its deviation is not significant. The present result does not require the existence of GZ events.

Edited by: T. Suomijarvi
Reviewed by: two anonymous referees

References

Zatsepin, G. T.: On the photodisintegration of heavy cosmic-ray particles by solar radiation, Dokl. Akad. Nauk. SSSR, 80, 577–578, 1951.

Gerasimova, N. M. and Zatsepin, G. T.: Splitting of cosmic ray nuclei by solar photons, ZhETF, 38, 1245–1252, 1960.

Medina-Tanco, G. and Watson, A.: The photodisintegration of cosmic ray nuclei by solar photons: the Gerasimova-Zatsepin effect revisited, Astropart. Phys., 10, 157–164, 1999.

Epele, L., Mollerach, S., and Roulet, E.: On the disintegration of cosmic ray nuclei by solar photons, J. High Energy Phys., 3, 17–31, 1999.

Fujiwara, Y., Iyono, A., Tada, J., et al.: Search for Simultaneous Parallel EAS Events in Long Baseline EAS Array with LAAS Nucl. Phys. B (Proc. Suppl.), 151, 481–484, 2006.

Lafebre, S., Falcke, H., Horandel, J., et al.: Prospects for direct cosmic ray mass measurements through the Gerasimova-Zatsepin effect Astron. Astrophys., 485, 1–4, 2008.

Akasofu, S. I., Gray, P. C., and Lee, L. C.: A model of the heliospheric magnetic field configuration, Planet. Space Sci., 28, 609–615, 1980.

Ochi, N. and Large Area Air Shower group: Search for large-scale coincidences in network observation of cosmic ray air shower, J. Phys. G: Nucl. Part. Phys., 29, 1169–1180, 2003.

Kitamura, T., Ohara, S., Konishi, T., et al.: Chaos in cosmic ray air showers, Atropart. Phys., 6, 279–291, 1997.

Amenomori, M., Ayabe, S., Bi, X. J., et al.: Moon shadow by cosmic rays under the influence of geomagnetic field and search for antiprotons at multi-TeV energies, Astropart. Phys., 28, 137–142, 2007.

Wang., Y. and the ARGO-YBJ Collaboration:, Preliminary results of the Moon shadow using ARGO-YBJ detector, Nucl. Phys. B (Proc. Suppl.), 175–176, 551–554, 2008.

The L3 Collaboration, Acharda, P., Adrianib, O., Aguilar-Benitez, M., et al.: Measurement of the shadowing of high-energy cosmic rays by the Moon: A search for TeV-energy antiprotons, Astropart. Phys., 23, 411–434, 2005.